

THE PASSAGE OF SHOCK WAVE THROUGH A PERMEABLE EXPLOSION DOOR - A COMPUTATIONAL STUDY

Michael Dwomoh & Darron Dixon

Department of Mechanical Engineering, Brunei University, Uxbridge, UK

I Göktaş Ediz

Department of Mining Engineering, Dumlupınar University, Kütahya, Turkey

ABSTRACT

In this paper the ability of an explosion door to withstand the force of an underground explosion was investigated. This was achieved by designing a computational model of a shock tube along which obstructions of various blockage ratios were tested.

Computationally, the shock tube was modelled using a two dimensional grid of about 32000 cells. Near the obstruction, the cells were distributed more densely. For this computational simulation, the blockage ratio for the obstruction was 50% of the shock tube diameter (55 mm) and was 50 mm in length. Though the shock tube problem is described an inviscid flow problem, with the obstruction in place, the k-e turbulence model was used.

The results show that an obstruction with a blockage ratio of 50% can reduce the strength of a shock wave with an incident pressure of over 0.3 MPa by about 50%.

1. INTRODUCTION

In an underground mining environment, the generation of methane is linked with the demand for an increase in productivity. This inevitably leads to the situation where the chances of a methane initiated explosion is enhanced. There are numerous ways of dealing with the methane generated during the mining of coal in an underground environment (Tuck and Dixon, 1993), however, as highlighted by Cybulska (1981), coal dust explosions still occur with devastating consequences. In most cases fatalities occur at locations further from the source of the explosion due to the effects of a methane initiated coal dust explosion that tends to propagate throughout the mine.

There are two main methods for arresting explosions (Liebman and Richard, 1978). Water barriers or stone-dust barriers have been used for several years with varying degrees of success. Depending on the severity of an explosion, these barriers might be unable to quench the explosion, leading to further damage and fatalities. In order to eliminate this problem, an explosion door acting as an additional barrier has been proposed, (Ediz et al., 1993).

Knowledge about the ability of the explosion door to withstand a shock wave and subsequently arrest the flame front would provide a useful design specification. This could then be used in the design, manufacture and installation of the explosion door in an underground environment.

Experimental and computational studies of the door are thus needed to prove its effectiveness. This paper presents the finding of a computational study of a shock wave propagating through a shock tube with and without the perforated barrier. This comparison is useful in that it shows the disturbance and pressure drop across the permeable barrier caused by the shock wave. The results have shown that a permeable barrier with the appropriate blockage ratio attenuates the strength of an incident shock wave by varying amounts depending on the blockage ratio and the incident pressure. The objective of the explosion door is to keep the attenuation to a minimum and remain structurally intact so that the following flame front can be successfully arrested.

2. COMPUTATIONAL FLUID DYNAMICS (CFD) STUDY

2.1 An Introduction to CFD

CFD is the analysis of systems involving fluid flow, heat transfer and associated phenomena such as chemical reactions by means of a computer based simulation. Thus it is the art of replacing the governing partial differential equations of fluid flow with numbers and advancing these numbers in space and/or time to obtain a final numerical description of the complete flow field of interest (Wendt, 1992). In short the aim of CFD is to predict fluid motion by solving the mass, momentum, and energy equations on a computational grid.

CFD codes are structured around the numerical algorithms that can solve fluid flow problems. There are three distinct streams of numerical solution techniques: finite difference, finite element and spectral methods. These methods solve the governing equations by performing the following steps:-

- Approximating the unknown flow variables by means of simple functions
- Discretising by substituting the approximations into the governing equations
- Solving the algebraic equations

The main differences between the numerical solution techniques are in the way in which the flow variables are approximated and with the discretisation processes. There are several CFD packages commercially available but for the purposes of this research, Rampant, supported by Fluent Europe was used for the computational work described in the following sections.

2.2 Shock Tubes - Background

Shock tubes are closed at both ends with a diaphragm separating a region of high pressure (4) from a region of low pressure (1).

The gases in regions (1) and (4) can be at different temperatures and have different molecular weights. In this research, an ideal gaseous media in both regions.

When the diaphragm is punctured using a solenoid, a shock wave propagates into region (1) and an expansion wave propagates into region (4). Figure 2.1 shows the initial conditions in a shock tube.

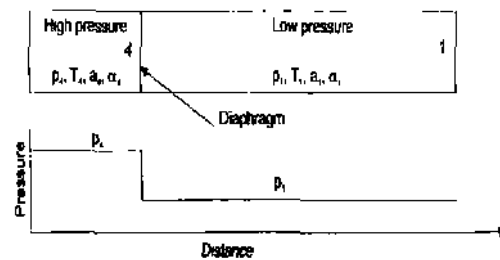


Figure 2.1 - Initial conditions in a pressure driven shock tube

In shock tubes, the flow field (which has properties dependent on both distance $\{x\}$ and time $\{t\}$) in the tube after the diaphragm is broken is determined by the given conditions in regions (1) and (4) before the diaphragm is punctured. The normal shock wave (representing an *unsteady wave motion*) propagates to the right with a velocity W , increasing the pressure of the gas behind it (region (2)), and inducing a mass motion with a velocity u_p (see Figure 2.2). The contact surface which is the interface between the driver and driven gases also moves with velocity u_s . Pressure and velocity are preserved across this contact surface but entropy changes discontinuously. The expansion wave propagates to the left (region (4)), smoothly and continuously decreasing in pressure to the lower value p_3 behind the expansion wave.

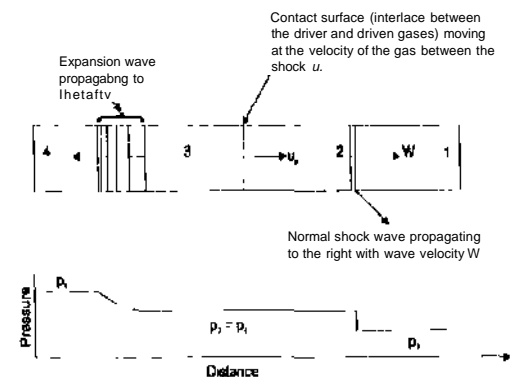


Figure 2.2 - Flow in a shock tube after the shock tube is broken.

2.3 Shock Wave Theory

When the diaphragm is punctured, a shock wave is generated which travels to the right (low pressure region) of the shock tube with a velocity W (region (1) ahead of the shock wave and relative to the wave. In region (2), the velocity of the gas behind the shock wave is $W - u_p$ relative to the wave. For regions (1) and (2) in the shock tube, the fluid flow must obey the equations for continuity, momentum, and energy for normal moving shock as the flow is akin to that of an unsteady moving shock wave (Anderson, 1990). These are:-

$$\rho_1 W = \rho_2 (W - u_p) \quad (1)$$

$$p_1 + \rho_1 W^2 = p_2 + \rho_2 (W - u_p)^2 \quad (2)$$

$$h_1 + \frac{W^2}{2} = h_2 + \frac{(W - u_p)^2}{2} \quad (3)$$

These equations yield the following equations, which determine the speed of the shock wave, and the incident shock strength respectively :-

$$W = a_1 \sqrt{\frac{\gamma + 1}{2\gamma} \left(\frac{p_2}{p_1} - 1 \right) + 1} \quad (4)$$

Equation (4) relates the wave velocity of the moving shock to the pressure ratio across the wave and the speed of sound into which the wave is propagating.

$$\frac{p_2}{p_1} = \frac{p_2}{p_1} \left[1 - \frac{(\gamma_1 - 1)(a_1/a_2)(p_2/p_1 - 1)}{\sqrt{2\gamma_1} \{2\gamma_1 + (\gamma_1 + 1)(p_2/p_1 - 1)\}} \right]^{\frac{2\gamma_1}{\gamma_1 - 1}} \quad (5)$$

Equation (5) gives the incident shock strength, p_2/p_1 as an implicit function of the diaphragm pressure ratio, p_2/p_1 .

2.4 CFD Modelling of a Shock Tube

The shock tube problem, which is a particular case of the more general Riemann problem (Hirsch, 1988), can be stated as follows:- given an inviscid, perfect gas at high pressure and another at low pressure, separated by a diaphragm in a tube of uniform cross

section, what type of flow is generated when the diaphragm is instantaneously removed? The Rampant CFD code describes this problem as a compressible emptying problem and is solved by designating the high pressure and low pressure regions with their appropriate pressure values. The permeable explosion door is then represented by an obstruction. However, the presence of an obstruction makes the flow turbulent.

2.5 Numerical Model

For turbulent flow, the original Navier-Stokes equations are decomposed into the mean, $\bar{\phi}$, and the fluctuating components, ϕ' . Thus $\phi = \bar{\phi} + \phi'$, where $\bar{\phi}$ denotes general scalars (pressure, velocity, enthalpy).

Substituting the expressions of this form for the flow variables into the instantaneous continuity and momentum equations and taking a time average (and dropping the overbar on the mean velocity, \bar{u}), the governing equations for turbulent flow are:-

Continuity Equation in the fth direction

$$\frac{\partial \rho}{\partial t} + \frac{\partial (\rho u_f)}{\partial x_f} = 0 \quad (6)$$

Momentum equation in the ith direction

$$\begin{aligned} \frac{\partial (\rho u_i)}{\partial t} + \frac{\partial (\rho u_i u_j)}{\partial x_j} = \\ \frac{\partial}{\partial x_j} \left[\mu \left(\frac{\partial u_i}{\partial x_j} + \frac{\partial u_j}{\partial x_i} \right) - \left(\frac{2}{3} \mu \frac{\partial u_l}{\partial x_l} \right) \right] \\ - \frac{\partial p}{\partial x_i} + \frac{\partial}{\partial x_j} (-\rho \overline{u'_j u'_i}) \end{aligned} \quad (7)$$

where p is the static pressure, u_i is the incompressible viscosity.

Equations (6) and (7) are known as the "Reynolds Averaged" Navier-Stokes equations. However, the effects of turbulence are represented by the correlation term, $-\rho \overline{u'_j u'_i}$. This term represents the diffusive transport of momentum by turbulent motion. These correlations need to be determined by a

turbulence model before the mean flow equations can be solved.

In Rampant (User's Guide, 1996) turbulence is modelled using "two-equation" turbulence models. In two-equation models, the effects of turbulence are represented by an isotropic "eddy" or "turbulent" viscosity which is evaluated using two quantities: turbulent kinetic energy (k) and its rate of dissipation (ϵ). The two turbulent quantities, k and ϵ , are obtained from the solutions of the "modelled" transport equations.

The turbulence models used in Rampant are :-

- * The $i-\epsilon$ model
- The ReNormalization Group (RNG) $k-\epsilon$ model

The latter model provides more accurate results over the standard $k-\epsilon$ model as it is derived by a more rigorous technique.

3. COMPUTATIONAL RESULTS

Figures 3.1 to 3.8 show the plots of fluid property along the length of the shock tube. Computationally, the pressure profile is similar to the ideal (inviscid flow) case, see Figure 2.2. With the obstruction in place, the flow becomes turbulent and is modelled as such.

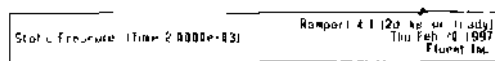
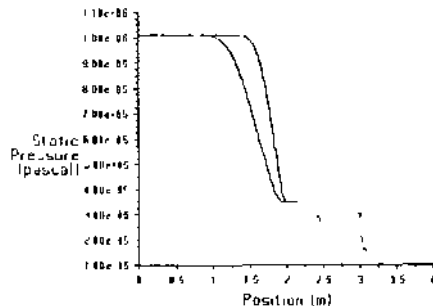


Figure 3.1 - Plot of static pressure along the shock tube

The graphs show a series of plots at time 1 ms, and 2 ms, with the diaphragm positioned at 2 m. When the diaphragm is punctured, the shock traverses to the

right hand side of the tube and the expansion traverses to the left hand side as can be observed in Figure 3.1 above.

The region in front of the first discontinuity represents region 1 where the fluid is still at rest. The discontinuity represents the shock wave with the region behind representing regions 2 and 3, where the pressure is conserved. As the shock wave propagates to the right, it increases the pressure of the gas behind it (region 2) and induces a mass motion with a velocity. The expansion wave propagates to the left, smoothly and continuously decreasing the pressure in region 4 to the lower value (p_4) behind the expansion wave. Region 4 is the high speed region with the pressure still at 10 bar.

At 2 ms, the shock has made contact with the obstruction and there is a pressure drop across it as shown in Figure 3.2 below. When compared with the pressure at 1 ms, the decrease in pressure can be attributed to the fact when the flow field meets the obstruction, the velocity increases through the restricted flow area.

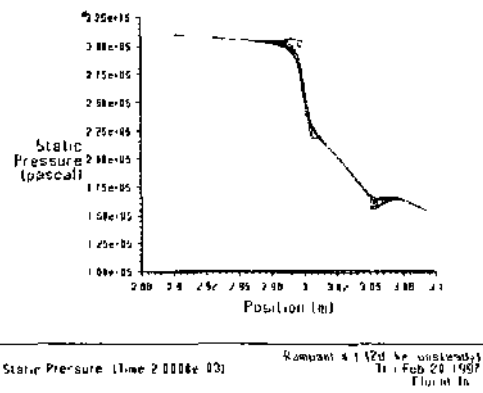


Figure 3.2 - Pressure drop across the obstruction in the shock tube

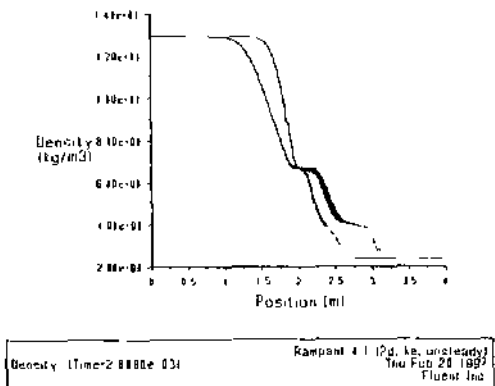


Figure 3.3 • Plot of density along the shock tube

Density also changes across the contact surface (Figure 3.3) since it is dependant on temperature as described by the equation given below:-

$$\rho = \frac{p_{op} + p}{RT_s} \quad (8)$$

where p_{op} is the operating pressure and p is the local static pressure relative to the operating pressure. R is the gas constant, and T_s is the temperature.

Across the obstruction, there is also a sharp drop in the value of density.

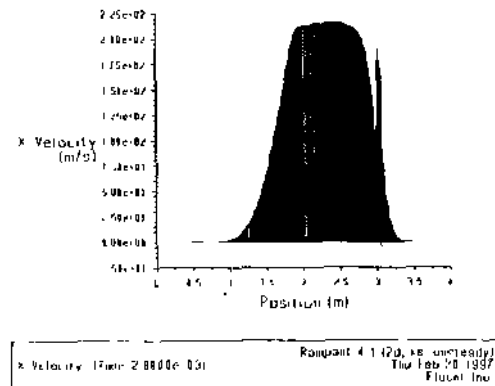


Figure 3.4 - Plot of X-velocity along the shock tube

The obstruction produces a sudden increase in the value of velocity (Figure 3.4) due to the decrease in the pressure. This is expected if continuity is to be maintained.

Figure 3.5 shows the nature of the flow field through the obstruction. There is a gradual decrease in the velocity until it reaches the obstruction at 3 m. There is then a sudden increase through the obstruction followed by a gradual decrease until the flow field exits the obstruction at 3.05 m. Upon exiting the obstruction, there is a gradual decrease in the value of the velocity.

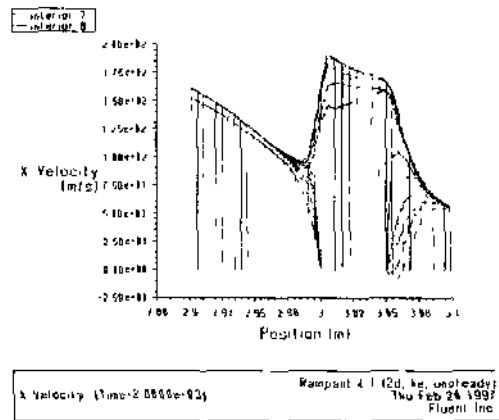


Figure 3.5 - Velocity drop across the obstruction

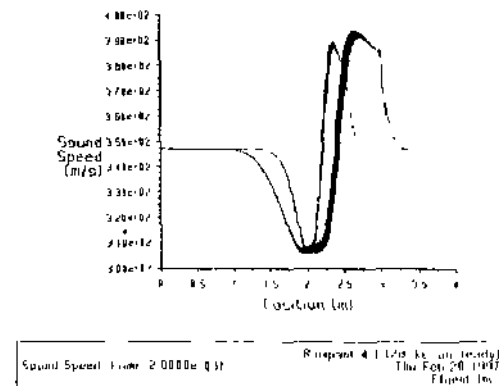


Figure 3.6 - Plot of shock speed along the shock tube

Behind the shock, the flow field induced by the passing shock is clearly travelling at a speed greater than the speed of sound (Figure 3.6). However, when the travelling shock meets the obstruction, there is a sudden drop in the value of the speed of sound. This is due to the fact that the speed of sound is dependent on temperature.

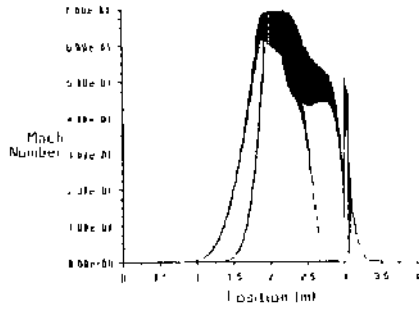


Figure 3.7 - Plot of mach number along the shock tube

Looking at the Mach number evolution from right to left (Figure 3.7), at 2 ms it has made contact with the obstruction and there is a sudden change in order to satisfy continuity. The sudden rise in Mach number can be attributed to the decrease in the sound speed and the increase in velocity of the flow through the obstruction. Upstream of the contact discontinuity, the smooth variation of all the flow properties represents the expansion waves.

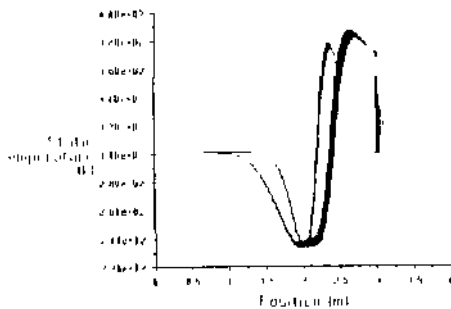


Figure 3.8 - Plot of static temperature along the shock tube

The discontinuity due to the shock can clearly be identified as it traverses the shock tube with time. However, as the region behind the shock (2) is acted upon by the shock and region 3 (Figure 2.2) is acted upon by an isentropic expansion wave, there is a difference in the temperature.

The change caused by the obstruction can be seen at 2 ms where there is steep change in temperature, with a sudden drop in the temperature.

4. CONCLUSION

Generally, due to the turbulent nature of the flow field, the discontinuity which is characteristic of a moving shock is not clearly defined in the plots, the continuity was however clearly defined when there were no obstructions and the flow could be described as an inviscid problem. This could be due to the fact that the discretisation scheme could not be changed when the flow was described as being turbulent in nature.

The purpose of this series of simulations were to determine the ability of an explosion door to withstand the blast of a shock wave emanating from an explosion. The above results are for an obstruction with a blockage ratio of 50% and a length of 50 mm situated at 3 m. At this position, the obstruction is 1 m from the diaphragm.

The plots above show that:-

- There is a sudden decrease in pressure when the shock wave meets the obstruction
- There is an increase in the mach number through the obstruction
- There are sudden changes in pressure and density. These changes result in a decrease in the values of these properties
- There is also a sudden change in temperature as the flow field meets the obstruction and exits with a lower value
- There is a rise in velocity of the flow field through the obstruction

The above points show that with an obstruction in place, the strength of explosion represented computationally by an incident shock wave of 0.3 MPa, is attenuated by 50%. This could be sufficient to not allow deformation of the explosion door and arrest the following flame front.

Further work will involve the evaluation of various blockage ratios and length of obstruction to determine optimum design criteria.

5. REFERENCES

Anderson, J. D. 1990. *Modern Compressible Flow - with Historical Perspective*. McGraw-Hill. ISBN 0071006656.

Cybulska, R. 1981. Examples of coal dust explosions. *Proc Aus. IMM Illawarra Branch: Ignitions, Explosions and Fires in Coal Mines Symposium*. (May): 7.1-7.13.

Ediz, I. G.; Gorgulu, A.; Dixon, D. W. 1993 A New Approach for Arresting the Propagation of Coal Dust Explosions - AGE 1. *Proceedings of the 13th Mining Congress of Turkey*. Istanbul, Turkey.

Hirsch, C. 1988. *Numerical Computation of Internal and External Flows - Volume 2: Computational Methods for Inviscid and Viscous Flows*. John Wiley & Sons. ISBN 0471923516.

Liebman, I; Richmond, J.K. 1978. Coal Dust Explosion Barriers. *Proceedings of the Bureau of Mines Technology Transfer Seminars on Coal Mine Fire and Explosion Prevention*, Pittsburgh and Denver. USBM IC 8768: 15-26.

Tuck, M. A.; Dixon, D. W 1993. Automatic Control of Mine Ventilation: Future Possibilities. *Journal of Mine Ventilation Society of South Africa*, Vol. 46 No. 10: 146-150. ISSN 03683206.

User's Guide for Fluent/Uns & Rampant, Release 4.0. 1996. Volume 3. Fluent Inc.

Wendt, J.F (ed.). 1992 *Computational Fluid Dynamics - An Introduction*. Springer-Verlag. ISBN 3-540-53460-1.

